Membrane Curvature and High-Field Electroporation of Lipid Bilayer Vesicles

Sergej Kakorin, Thomas Liese, and Eberhard Neumann*

Physical and Biophysical Chemistry, Faculty of Chemistry, University of Bielefeld, Germany

Received: October 23, 2002; In Final Form: June 30, 2003

The turbidity relaxations of small unilamellar lipid vesicles, vesicle radii a/nm = 25, 38, 80, and 170, prepared from commercial 20% (weight) lecithin in 0.2 mM NaCl aqueous solution exposed to a rectangular field pulse of field strengths in the range $0 < E/\mathrm{MV\ m^{-1}} \leq 8$ indicate vesicle electro-elongation coupled to smoothing of membrane thermal undulations and membrane stretching as well as membrane electroporation (MEP). If compared at the same nominal transmembrane potential, here $\Delta\varphi^{N} = -1.5Ea = -0.3$ V, at the pole caps and at zero membrane conductivity, the decrease in the vesicle radius leads to an increase in the fraction $f_p = \Delta S_p/S_0$ of porated membrane area from $f_p = 1.0 \times 10^{-3}$ at $a = 170$ nm to $f_p = 2.9 \times 10^{-2}$ at $a = 25$ nm. The effect of the membrane curvature on MEP is specified in terms of the difference in the lipid packing density in the outer and inner membrane leaflets. The formation of one mole of pores of mean radius $\bar{r}_p = 0.35 \pm 0.05$ nm is accompanied with the dissipation of the molar area difference elasticity energy of $\Delta_r G_{ADE} = -3.2RT$ at the vesicle radius $a = 25$ nm and of $\Delta_r G_{ADE} = -0.5RT$ at $a = 170$ nm, where R is the gas constant and $T = 293$ K (20 °C). In brief, membrane curvature favors electric pore formation.

Introduction

The electrical and mechanical properties of biological membranes scale well with those of artificial lipid bilayers.[1] In this sense, also the electrodeformation of lipid bilayer vesicles provides information for the understanding of the electromechanical behavior of biological cells in electric fields.[2,3] Previously, the deformation of lipid vesicles in longer lasting AC−electric fields has been quantified using micrographic contours of electrodeformed giant vesicles in the radius range of $5 \leq a/\mu\mathrm{m} \leq 10$.[4] Recent progress in processing and interpreting electric light scattering data of smaller lipid vesicles of a/nm = 25−170 in short-duration electric fields[3] is the basis for understanding the electro-elongation of small vesicles in terms of specific membrane properties.

The large curvature of small vesicles is associated with a density gradient of lipid molecules along the membrane normal.[5] Therefore, characteristic membrane properties such as bending rigidity (κ), compression modulus (K), as well as extent and rate of membrane electroporation (MEP) are expected to be different for large, as compared to small, vesicle radii. Recently, it has been concluded from the extent and rate of MEP that the spontaneous membrane curvature facilitates MEP.[6] Analogous to Helfrich's spontaneous curvature, it has been conjectured that the "geometrical" curvature of the membrane in the pole caps of elongated vesicles may increase the extent and the rate of MEP.[7,8]

The deformational response of vesicles to electric fields reflects complex processes including smoothing of membrane undulations, membrane stretching, as well as MEP.[3] Fortunately, the different kinetic time scales of membrane smoothing and MEP permit to analyze these processes separately. By varying the field strengths E at different radii a, satisfying the condition Ea = constant, the effect of the membrane curvature on MEP has been quantified for a constant transmembrane potential $\Delta\varphi_m$ across the vesicle bilayer, i.e., for a constant membrane field $E_m = |\Delta\varphi_m|/d$, where d is the membrane thickness.

Material and Methods

1. Vesicle Suspensions. Unilamellar phospholipid vesicles have been prepared by the extrusion method (see, e.g., ref 9), using the commercial chloroform/methanol lipid extract of 20% (weight) lecithin (also called Soy 20 or Avanti 20) kept deep-frozen at −80 °C. The purified extract contains 20 (weight) % phophatidylcholine (PC), 10% phosphatidic acid (PA), 30% phophatidylethanolamine (PE), 20% phophatidylinositol (PI), and 20% other not specified lipids from Avanti Polar Lipids. The electrooptic data of a mixture of synthetic lipids at similar conditions of lipid concentration, buffer, and temperature[9] are similar to those described here (for Avanti 20).

The vesicle mean diameters ∅ = 50, 76, 160, and 340 nm have been determined by dynamic light-scattering measurements (data not presented). All samples are suspended in aqueous 0.2 mM NaCl solution and measured immediately after preparation. The final total lipid concentration used for the electrooptical measurements is $[L_T] = 1$ mM, corresponding to a vesicle number density of $\rho_v \approx 10^{14}-10^{16}$ dm^{-3}, depending on ∅. Under these conditions, the average distance between the surfaces of single vesicles in all cases is larger than the diameter, qualifying the suspension as diluted with practically no vesicle−vesicle contacts, also during the short field pulse.[10]

2. Electrooptical Relaxations. Rectangular pulses of field strengths of up to $E = 8$ MV m^{-1} and of duration of $t_E = 10$ μs are applied by cable discharge to the sample cell equipped with parallel planar graphite electrodes, thermostated at $T = 293.0 \pm 0.1$ K (20 °C). The field-induced changes in the transmittance of plane-polarized light is measured at the wavelength $\lambda = 365$ nm (Hg-line; highest accuracy).

The light intensity change ΔI^{σ}, caused by the electric pulse and measured at the polarization angle σ relative to the direction

* To whom correspondence should be addressed. Phone: +49 521 106 20 53. Fax: +49 521 106 29 81. E-mail: eberhard.neumann@uni-bielefeld.de.

10.1021/jp022296w CCC: $25.00
Published on Web 08/26/2003

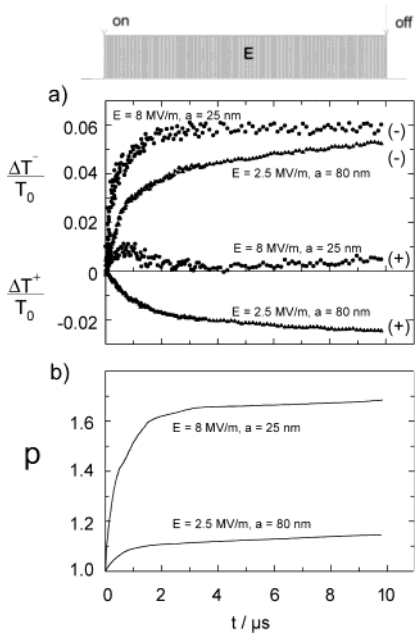

Figure 1. Digitized high-field electrooptical relaxation modes in the presence of the electric field. (a) The minus (−) mode $\Delta T^{-}/T_0 = (\Delta T^{\parallel} - \Delta T^{\perp})/T_0$ and the plus (+) mode $\Delta T^{+}/T_0 = (\Delta T^{\parallel} + 2\Delta T^{\perp})/(3T_0)$ of the turbidity changes ΔT^{σ} at the parallel ($\sigma = \parallel$) and the perpendicular ($\sigma = \perp$) light polarization modes ($\lambda = 365$ nm) relative to the zero field turbidity T_0, respectively, and (b) the total axis ratio $p = c/b$ of the elongated vesicles, all as functions of time t: (▲) at the field strength $E = 2.5$ MV m^{-1} and the vesicle radius $a = 80$ nm, (●) at $E = 8$ MVm^{-1} and $a = 25$ nm. Unilamellar lipid vesicles in dilute suspension, internal and external [NaCl] = 0.2 mM at the total lipid concentration [LT] = 1.0 mM, are exposed to a rectangular electric field pulse of the duration $t_E = 10$ μs at $T = 293$ K (20 °C).

of the applied external field vector E, is related to the optical density change by $\Delta OD^{\sigma} = OD^{\sigma}(E) - OD_0^{\sigma} = -\log(1 + \Delta I^{\sigma}/I^{\sigma})$, where $\Delta I^{\sigma} = I^{\sigma}(E) - I^{\sigma}$ is the light intensity change from I^{σ} (at $E = 0$) to I^{σ}(E) in the presence of E. $OD^{\sigma}(E)$ and OD_0^{σ} are the optical densities at E and at $E = 0$, respectively. Generally, $OD = A + T$, comprising both absorbance (A) and turbidity (T) along the light path length $l = 1$ cm. In our case, we have $A \ll T$; therefore, $\Delta OD^{\sigma} = \Delta T^{\sigma}$. The field induced changes $\Delta T^{\parallel}$ and $\Delta T^{\perp}$ at the two light polarization modes $\sigma = 0°$ ($\parallel$, parallel to the external field vector $\vec{\mathbf{E}}$) and $\sigma = 90°$ ($\perp$, perpendicular to $\vec{\mathbf{E}}$) are given by $\Delta T^{\parallel} = T^{\parallel} - T_0$ and $\Delta T^{\perp} = T^{\perp} - T_0$, respectively.

Generally, the difference (or minus) mode $\Delta T^{-} = \Delta T^{\parallel} - \Delta T^{\perp}$ *is not the classical dichroism* ΔT. There are usually contributions from nonorientational processes, characterized by the turbidity plus term $\Delta T^{+} = (\Delta T^{\parallel} + 2\Delta T^{\perp})/3$,[11] covering changes in the scattering cross section due to entrance of water and ions into the electroporated lipid membrane as well as changes of the vesicle volume. Proper analysis of field effects requires *both* ΔT^{-} *and* ΔT^{+}.

Experimental Results and Theory

1. Determination of Vesicle Deformation from Optical Density Changes. A spherical lipid vesicle elongated in an electric field is modeled by an ellipsoid of revolution with the principal semi-axes c and b, $c > b$. During the field pulse, the longest axis c of the ellipsoids is parallel to the external field direction.[3] Computer processing of the $\Delta T^{-}/T_0$ and the $\Delta T^{+}/T_0$ turbidity modes (Figure 1a) with a Mie-type numerical code[12] yields the total degree of the vesicle elongation expressed by the axis ratio $p = c/b$ as a function of time (Figure 1b).

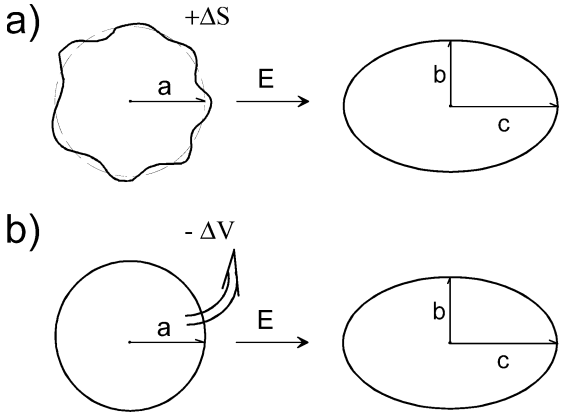

Figure 2. Short-time/low-field electroelongation of small lipid bilayer vesicles. (a) Increase in the surface membrane area $\Delta S = S - S_0 = \Delta S_{ss} + \Delta S_p$ of undulated membranes by stretching and smoothing of thermal undulations (ΔS_{ss}) and by membrane electroporation (ΔS_p). The dashed line represents the projected surface area $S_0 = 4\pi a^2$ of the undulated total area $S = S_0 + \Delta S_{ss} + \Delta S_p$ at $E = 0$. (b) Reduction of the intravesicular volume ($-\Delta V$) by efflux of electrolyte through electropores.

Theoretically, an elongation of a spherical vesicle must be accompanied either by an increase in the membrane surface area ΔS (by smoothing of undulations, membrane stretching, and electroporation), by a decrease of the intravesicular volume ΔV due to efflux of internal medium through the membrane pores), or with both (Figure 2).

Conductometric data of salt-filled vesicles have shown,[13] however, that in the case of vesicles with equal electrolyte concentration in the bulk and in the vesicle interior, the volume change during the short electric pulse duration $t_E = 10$ μs can be neglected. Therefore, the degree of vesicle elongation is concomitant with the increase $\Delta S = S - S_0$ in the membrane area, where $S_0 = 4\pi a^2$ is the projected membrane surface area at $E = 0$ and S is the membrane area in the field E (Figure 2 a). The relative increase $\Delta S/S_0$ at constant volume is readily expressed in terms of the axis ratio p by eq A5 of the Appendix.

2. Thermal Undulations and Stretching of Membranes. Due to the thermal motion, fluid membranes such as the lipid bilayers of unilamellar vesicles undergo out-of-plane fluctuations, called undulations. In large vesicles of very small membrane lateral tension σ, the undulations are visible in the light microscope.[14] Flaccid-stressed state transitions of smaller nanometer-vesicles (Figure 2a) cannot be observed in the microscope. However, such field-induced transitions can be derived from the kinetics of the membrane area increase during vesicle electroelongation in the μs time range. The fractional increase of the area $\Delta S_{ss}/S_0$ due to membrane stretching and smoothing of thermal undulations is given by[15]

$$\frac{\Delta S_{ss}}{S_0} = \frac{\sigma}{K} + \frac{k_B T}{8\pi\kappa}\cdot\left[\ln\left(\frac{S_0}{s}\right) - \ln\left(\frac{\pi^2/s + \sigma/\kappa}{\pi^2/S_0 + \sigma/\kappa}\right)\right] \qquad (1)$$

where K (N m^{-1}) is the membrane stretching modulus, κ (J) the membrane bending rigidity, k_B the Boltzmann constant, T the absolute temperature, and $s \approx 0.5$ nm^2 is the mean area of the cross section of a lipid molecule in the membrane.[16] The first term on the right-hand side of eq 1 accounts for the real stretching of the membrane under the action of the lateral surface tension σ, the second one stands for an increase in S due to the smoothing of membrane undulations. Vesicle deformation at constant volume leads to an increase $\Delta\sigma = \sigma - \sigma_0$ in the lateral membrane tension, reducing thermal undulations and increasing

the projected area by ΔS. Generalization of eq 1 to the case of a finite initial tension σ_o (at $E = 0$) yields

$$\frac{\Delta S}{S_o} = \frac{\Delta\sigma}{K} + \frac{1}{L}\ln\left[\frac{\pi^2/s + \sigma_o/\kappa}{\pi^2/s + (\sigma_o + \Delta\sigma)/\kappa} \cdot \frac{\pi^2/S_o + (\sigma_o + \Delta\sigma)/\kappa}{\pi^2/S_o + \sigma_o/\kappa}\right] \quad (2)$$

where $L = 8\pi\kappa/(k_B T)$ is a dimensionless quantity.

For most cases of practical interest, we may use the inequalities

$$\frac{\pi^2}{s} \gg \frac{\sigma_o + \Delta\sigma}{\kappa} \gg \frac{\pi^2}{S_0} \quad (3)$$

and eq 2 simplifies to

$$\frac{\Delta S}{S_0} = \frac{\Delta\sigma}{K} + \frac{1}{L}\ln\left[1 + \frac{\Delta\sigma}{\sigma_o}\right] \quad (4)$$

The solution of eq 4 with respect to $\Delta\sigma$ yields

$$\Delta\sigma = \frac{K}{L}\cdot\text{LambertW}\left[\frac{L}{K}\sigma_o \exp\left[\frac{L}{K}\left(\frac{\sigma_o}{K} + \frac{\Delta S}{S_0}\right)\right]\right] - \sigma_o \quad (5)$$

where LambertW is a special function (see, e.g., ref 11).

If the inequality $\Delta\sigma/\sigma_o \ll 1$ holds, only the term of the first power in $\Delta\sigma/\sigma_o$ is relevant in the expansion of the logarithm in eq 4 which then reduces to

$$\frac{\Delta S}{S_0} = \Delta\sigma\left[\frac{1}{K} + \frac{1}{L\sigma_o}\right] \quad (6)$$

Rearrangement of the eq 6 with respect to $\Delta\sigma$ gives

$$\Delta\sigma = \frac{\Delta S}{S_0} \cdot \frac{K}{1 + \frac{K}{L\sigma_o}} \quad (7)$$

The degree p_o of the equilibrium vesicle deformation is found by minimizing the Gibbs energy density difference $\Delta g = g(E) - g(0)$ per unit membrane area between the two vesicle states: "0" at $E = 0$ and "E" at $E > 0$. Explicitly, we obtain

$$\Delta g = \Delta g_{\text{field}} + \Delta g_{\text{bend}} + \Delta g_{\text{ss}} \quad (8)$$

where Δg_{field}, Δg_{bend}, and Δg_{ss} refer to the contributions of electric field, bending, and stretching−smoothing, respectively. See eqs A1−A3 of the Appendix. If eq 5 applies, the equilibrium value of p_0 can be calculated numerically by finding a minimum of eq 8 according to $(\mathrm{d}(\Delta g)/\mathrm{d}p)|_{p=p_0} = 0$ at $p = p_0$. In the case where eq 7 applies, p_o is approximated by

$$p_o \approx \frac{3\epsilon_o\epsilon_w E^2 a^3}{62\kappa + 10\sigma_o a^2\left(1 + \frac{K}{\sigma_o + K/L}\right)} + 1 \quad (9)$$

The validity of eq 9 can be shown for the parameter range in eq 3. See eq A12 of the Appendix.

3. Characteristic Time of Vesicle Elongation. If the approximation of eq 7 applies, the characteristic time τ of the vesicle deformation can be estimated by integration of the Stokes equation; see eq A14 of the Appendix. From eq A15 we readily derive

$$\tau \approx \frac{3\eta a^3}{\frac{48\kappa}{5} + \frac{3}{2}\sigma_o a^2\left(1 + \frac{K}{\sigma_o + K/L}\right)} \quad (10)$$

Equation 10 correlates well with the expression for the characteristic relaxation time of the out-of-plane displacement modes of spherical fluid vesicles.[17] In the limiting case of $\sigma_o = 0$, eq 10 is reduced to the approximation

$$\tau = 0.38\eta a^3/\kappa \quad (11)$$

Equation 11 represents the upper limit of the shape relaxation time of a deformed sphere.[15] Note that in the range of validity of eq 11, i.e., small vesicle elongation ($p < 1.1$), the characteristic time is *independent* of the field strength. At larger p, however, the electric Maxwell stress on the vesicle depends on p; therefore, τ becomes a function of the field strength E. See also ref 18. For the common case of eq 5, the eq A15 can be used to calculate τ, generally.

Data Analysis and Discussion

1. Data Base. In the range of vesicle radius $25 \le a/\text{nm} \le 170$ and in the field strength range $8 \ge E/\text{MV m}^{-1} \ge 1.2$, the ΔT^- turbidity relaxations are positive, reflecting vesicle electroelongation in the direction of the field vector E (Figure 1a). The plus turbidity mode (ΔT^+) strongly depends on the vesicle size. For example, at $a = 25$ nm, ΔT^+ is positive and very small. For larger vesicle radii, $38 \le a/\text{nm} \le 170$, the ΔT^+ relaxations become negative. The ΔT^+ data are consistent with entrance of water into the lipid headgroup region of the membrane[3] and not with a reduction of the intravesicular volume.

The conductometric data of salt-filled lecithin (20%) vesicles, $a = 80$ nm, for instance at $\Delta\varphi^N = -0.3$ V, indicate that there is no volume reduction at $E = 2.5$ MV m^{-1} and $t_E = 10$ μs,[13] consistent with the case of non-salt-filled vesicles at the same $\Delta\varphi^N = -0.3$ V, where the electrolyte efflux through electropores is negligibly small. Therefore, there is no volume reduction, yet at $a = 25$ nm and the large field $E = 8.0$ MV m^{-1} the vesicles are strongly elongated ($p = 1.68$). Note that the ΔT^+ relaxation is positive and small (Figure 1a). At larger vesicle radii, the negative sign of ΔT^+ mode is solely due to a field-induced decrease in the average refractive index n of the membrane.

At $a = 25$ nm, the low lipid packing causes an already initially larger water content of the membrane, which hardly can be further increased by the field, hence the very small amplitude of ΔT^+. On the other hand, at larger vesicle radii, $38 \le a/\text{nm} \le 170$, the initially low water content in the more densely packed lipid membrane can be increased by the electric field. Since the refractive index $n \approx 1.484$ of pure lipid membrane is larger than that of water $n_w = 1.333$, the entrance of water in the membrane phase leads to negative values of the ΔT^+ mode.

The initial values T_0 of the turbidity (data not presented) are consistent with a 6% increase in the refractive index of the membrane from $n = 1.400$ at $a = 25$ nm up to $n = 1.484$ at $a = 170$ nm. This reflects, too, that the less dense lipid packing order in small vesicles and the larger water content result in a smaller effective refractive index. Both the difference in the refractive indices of vesicles of different sizes and the decrease in the index during the pulse must be included in the calculation of the axis ratios p (Figure 1b).

Substitution of the p values into eq A5 yields the relative increase $\Delta S/S_0$ in the membrane surface area. The time cause

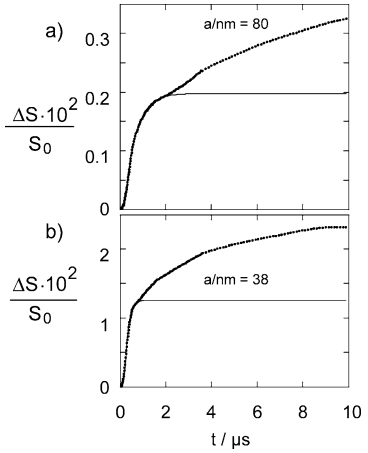

Figure 3. Surface area relaxations calculated with eq A5 from the axis ratios p (see, e.g., Figure 1b). The total relative increase $\Delta S/S_0$ in the vesicle surface area as a function of time t (a) at the vesicle radius $a = 38$ nm and the field strength $E = 5.3$ MV m^{-1} and (b) at $a = 80$ nm and $E = 2.5$ MV m^{-1}. The solid lines in (a) and (b) are the theoretical simulations of the relative increase $\Delta S_{ss}/S_0$ in the surface area due to membrane stretching and smoothing of thermal undulations.

TABLE 1: Axis Ratio $p = c/b$, Curvature-Equivalent Radius $a_{eq} = 2/\langle H\rangle$, Relative Increase $\Delta\langle H\rangle/\langle H_0\rangle$ in the Average Membrane Curvature and the Relative Decrease $\Delta K_p^0/K_p^0 = \Delta f_p/f_p$ in the Equilibrium Constant of Pore Formation at Different Vesicle Radii a and Field Strengths E[a]

E/MV m^{-1}	a/nm	a_{eq}/nm	$\Delta\langle H\rangle/\langle H_0\rangle$	$\Delta K_p^0/K_p^0$	p
1.2	170	169.9	0.0004	−0.012	1.05
2.5	80	79.9	0.0016	−0.029	1.10
5.3	38	37.4	0.015	−0.062	1.35
8.0	25	23.9	0.044	−0.092	1.68

[a] Comparison refers to the same membrane field, here $Ea = 0.2$ V.

of $\Delta S/S_0$ consists of two phases: a rapid one with the characteristic time $\tau_I < 1$ μs and a slow phase with $\tau_{II} \gg 1$ μs (Figure 3a,b). Since the characteristic times of electric polarization, stretching, and smoothing of membrane undulations, respectively, are usually very small ($\tau_{ss} \leq 1$ μs),[3] the increase in $\Delta S/S_0$ after 1 μs must be caused by membrane electroporation. Visual inspection of the data (Figure 3a,b) shows that the slow phase is apparently delayed relative to the rapid one. This delay permits to readily determine the amplitude $\Delta S_{ss}/S_0 = \Delta S(p_0)/S_0$ of the rapid phase, because the first phase approaches a saturation value before the second phase starts to increase. For the analysis of the effect of membrane curvature on MEP, i.e., on $f_p = \Delta S_p/S_0$, we use the same nominal transmembrane potential $\Delta\varphi^N = -1.5Ea = -0.3$ V, referring to the vesicles' pole caps at zero membrane conductivity.[9] In this way, any radius dependence refers to the same membrane field $E_m = -\Delta\varphi^N/d$, where $d = 5$ nm. Practically, the field strengths and radii have been chosen such that the condition $Ea = 0.2$ V is satisfied (see Table 1). At the same $\Delta\varphi^N = -0.3$ V, the amplitude and the rate of the f_p relaxations steeply decrease with increasing a (Figure 4), suggesting that it is MEP that is strongly affected by the membrane curvature H. The increase in H during vesicle elongation is relatively small.

2. Data Analysis. Vesicle Elongation Due to Membrane Stretching and Smoothing. In the data range defined by $Ea = 0.2$ V the maximum increase $\Delta\sigma = a\Delta P/4 = (3/80)a\epsilon_o\epsilon_w E^2$ of the lateral membrane tension induced by the electric Maxwell stress is small, $\Delta\sigma \leq 42$ μN m^{-1}; hence, eq 3 holds. The factor 4 in the Laplace expression $\Delta\sigma = a\Delta P/4$ refers to the two water−lipid interfaces of the vesicle membrane, whereas for a water droplet in the gas phase $\Delta\sigma = a\Delta P/2$. However, even for the maximum experimental value $\sigma_0 = 0.5$ μN m^{-1} of the initial lateral membrane tension for phospholipid vesicles,[4] the inequality $\Delta\sigma/\sigma_o \ll 1$ is not fulfilled. Therefore, the exact eq 5 is applied to calculate the axis ratio p_0. However, at constant values of κ, K, and σ_0, the exact numerical calculations with eq 5 cannot describe the experimental data in the entire radius range; see the dashed lines in Figure 5a. Nevertheless, the data are consistent with an increase in κ and in $K = 48\kappa/d^2$ [19] with increasing radius in the ranges: $2.95 \leq \kappa/10$,[20] $J \leq 11.5$, and $0.06 \leq K/\text{N m}^{-1} \leq 0.22$ for the radius range $25 \leq a/\text{nm} \leq 170$, respectively (Figure 5b).

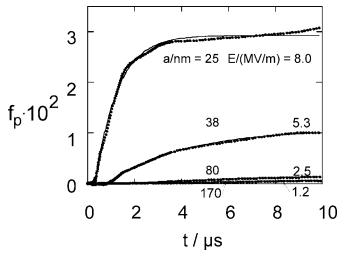

Figure 4. The relative increase $f_p = \Delta S_p/S_0 = (\Delta S - \Delta S_{ss})/S_0$ in the vesicle surface area due to formation of membrane electropores as a function of time t at different pairs of vesicle radius and field strength: a (nm)/E (MV m^{-1}) = 25/8; 38/5.3; 80/2.5, 170/1.2, respectively, i.e., for the same nominal transmembrane potential, here $\Delta\varphi^N = -1.5Ea = -0.3$ V.

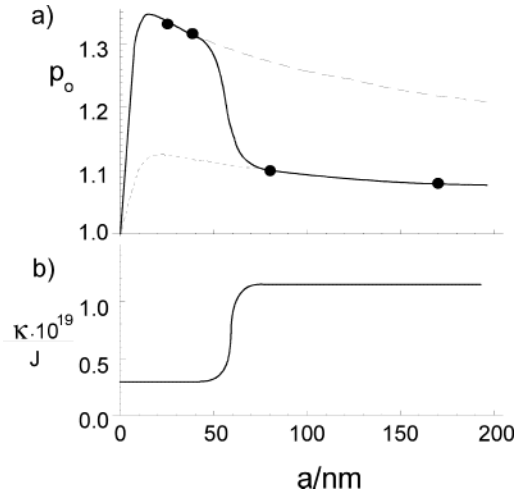

Figure 5. Vesicle radius dependencies of (a) the equilibrium axis ratio p_o and (b) the bending rigidity κ, both as a function of the vesicle radius a at the same transmembrane potential $\Delta\varphi^N = -1.5aE = -0.3$ V: (●), experiment, $p_o = p(10\ \mu s)$. The upper dashed curve is calculated using the exact eq 5 with $\kappa = 2.95 \times 10^{-20}$ J, $K = 0.06$ N m$^{-1,}$ and $\sigma_o = 0.5$ μN m^{-1}. The lower dashed curve refers to $\kappa = 11.5 \times 10^{-20}$ J, $K = 0.22$ N m$^{-1,}$ and $\sigma_o = 0.5$ μN m^{-1}. The solid curve in (a) is calculated with κ, which increases with the radius as shown in (b).

Since the relative increase $\Delta S_{ss}/S_0 \approx (8/45)(p-1)^2$ in the membrane area is a quadratic function of $(p-1)$,[3] the characteristic time τ_{ss} of the stretching and smoothing relaxations is approximately $\tau_{ss} \approx 2\tau$, where τ is the characteristic time of vesicle elongation given by eq 10. For the case of a radius-dependent value of κ (Figure 5b), the time constant τ_{ss} increases nonlinearly with increasing a (Figure 6). The characteristic time τ_{pol} of the electric membrane polarization can be calculated by $\tau_{pol} = 1.5aC_m\lambda^{-1}$, where $C_m = 0.56 \times 10^{-2}$ F m^{-2} is the specific

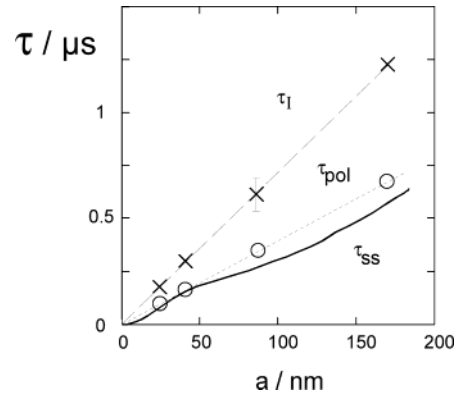

Figure 6. Radius dependence of the time constants: (×) the characteristic time τ_I of the first phase $\Delta S_{ss}/S_0$ of the relative total increase $\Delta S/S_0$, due to membrane stretching and smoothing of thermal undulations (see Figure 3a,b) at the same nominal transmembrane potential $\Delta\varphi^N = -1.5aE = -0.3$ V; (○) characteristic time τ_{pol} of the electric membrane polarization. The solid line refers to the characteristic time $\tau_{ss} = 2\tau$ of membrane stretching and smoothing of thermal undulations, calculated with eq A15 and Mathematica 4 package.

membrane capacitance, $\lambda = \lambda_{in} = \lambda_{out} = 2 \times 10^{-3}$ S m^{-1} is the conductivity of vesicle interior and that of the bulk at [NaCl] = 0.2 mM,[20] respectively. Here, the two time constants τ_{ss} and τ_{pol} are similar in value (Figure 6). The comparatively large value of τ_{pol} leads to a distinct delay in the first phase of $\Delta S_{ss}/S_0$ (Figure 3a,b). Kinetic analysis of the $\Delta S_{ss}/S_0$ relaxations shows that the total characteristic time τ_I of the first phase (together with delay) is practically the sum $\tau_I = \tau_{ss} + \tau_{pol}$. This fact is in line with the convolution of the electric polarization with the process of membrane stretching and smoothing. This quantifies the rapid phase of the total area increase as being dominantly due to membrane stretching and smoothing of thermal undulations.

Elongation of Small Vesicles Due to Membrane Electroporation. The formation of small water-filled membrane electropores inevitably leads to an additional increase in the overall membrane surface area by $\Delta S_p = N_p \pi \bar{r}_p^2$, where N_p is the number of pores per vesicle and $\bar{r}_p$ is the mean pore radius. It is recalled that this increase ΔS_p is kinetically delayed relative to ΔS_{ss} (Figure 3). Obviously, the elongation of vesicles due to membrane stretching and smoothing leads to an increase in the membrane curvature in the pole caps. Such a curvature increase was conjectured to facilitate MEP.[7,8] However, at the maximum $p = 1.68$ for $a = 25$ nm, the relative θ-average increase $\Delta\langle H\rangle/\langle H_0\rangle$ in the membrane curvature does not exceed 4.2%; see eq B5 of the Appendix and Table 1. Therefore, the spherical approximation for the membrane curvature $\langle H\rangle \approx H = 2/a$ applies and the small values of $\Delta\langle H\rangle/\langle H_0\rangle$ during vesicle elongation permit to treat the membrane elastic parameters κ and K as constants, independent of p. Actually, $\Delta\langle H\rangle/\langle H_0\rangle = 0.042$ is equivalent to a decrease of the vesicle radius from $a = 25$ nm to $a_{eq} = 23.9$ nm (Table 1). This decrease is still within the error margin of the experimental data (±5%), such that there is practically no change in κ and K (Figure 5b).

Since at $\Delta\varphi^N = -0.3$ V, the time constant τ_p of MEP is usually a few microseconds,[13,21] the slow second phase of the ΔS relaxation is also kinetically consistent with the electroporative increase (ΔS_p) in the membrane area (Figure 4).

It has been reported that giant vesicles of $a = 11.25$ μm at high field strengths corresponding to $\Delta\varphi^N = -1.86$ V and large pulse duration $t_E = 0.7$ ms do not show visible elongation. At this high voltage and long pulse duration there is a "loss of up to 14% of lipid membrane" from the originally larger vesicles.[22]

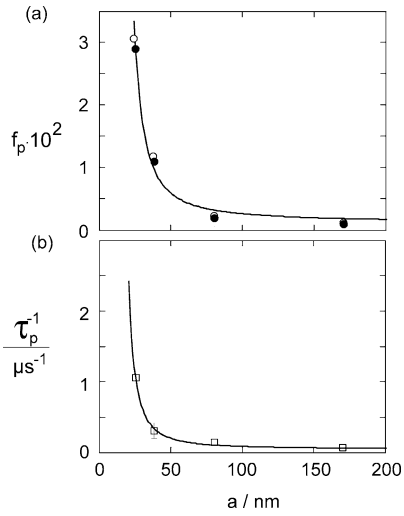

Figure 7. Radius dependencies of the relaxation modes. (a) Amplitudes of the $f_p = \Delta S_p/S_0$ relaxations: (●) actually measured values for elongated vesicles; (○) corrected values for the equivalent spherical vesicle at the same $\Delta\varphi^N = -1.5aE = -0.3$ V; see eq B5 and eq C5 of the Appendix. The solid curves represent the data fit by $f_p = K_p^0 \exp(B_H a^{-1})$ with $K_p^0 = 1.2 \times 10^{-3}$ and $B_H = 81$ nm^{-1}. (b) Relaxation rates $\tau_p^{-1} = \tau_{II}^{-1}$ (□) of the $f_p = \Delta S_p/S_0$ relaxations at $\Delta\varphi^N = -1.5aE = -0.3$ V. The solid curves represent the data fit by $\tau_p^{-1} = \tau_0^{-1} \exp[b_H a^{-1}]$ with the parameters $\tau_0^{-1} = 0.037$ μs^{-1} and $b_H = 84$ nm^{-1}.

Obviously, giant lipid vesicles at low voltages behave differently. Visibly, they remain apparently spherical but the size is reduced, probably caused by bleb formation and abstraction of smaller vesicles.

It is known that the field-induced Maxwell stress can lead to different types of shape changes, depending on vesicle size and the electrical pulse conditions. Equation 10 shows that the elongation time constant depends on a^3. For $a = 11.25$ μm, we estimate $\tau = 1.7$ s; for $a = 80$ nm, we obtain $\tau = 0.6$ μs (Figure 6). Because of the large elongation time constant of giant vesicles, the local effect of bleb formation is obviously faster and precedes a possible global shape elongation. In this context various other shape changes such as local volcano structures (20−120 nm in diameter) have been observed in red blood cells, when osmotic gradients of hemoglobin molecules exist during and after pulse application.[23]

Electroporative Increase in Membrane Area Is Facilitated by Curvature. The dramatic effect of the membrane curvature ($H = 2/a$) on the degree of poration ($f_p = \Delta S_p/S_0$), here demonstrated for $\Delta\varphi^N = -0.3$ V (Figure 7 a), can be readily rationalized with the concept of the area-difference-elasticity (ADE) Gibbs energy,[24] which already has been successfully applied to describe the effect of adsorbed human annexin V on MEP of lipid vesicles.[9] The curvature of the vesicle membrane is associated with different packing densities of the lipid molecules in the outer and in the inner leaflets of the bilayer, respectively, corresponding to different lateral pressure in the two monolayers. The gradient in the lateral pressure across the vesicle membrane can be reduced by the formation of (conical) electropores. The molar ADE reaction Gibbs energy for the pore formation is given by[9]

$$\Delta_r G_{ADE} \approx -\frac{64\pi^2 \alpha \kappa \bar{r}_p^{\,2} \xi N_A}{d} a^{-1} \qquad (12)$$

The negative sign indicates release (or dissipation) of Gibbs energy upon pore formation. In eq 12, N_A is the Avogadro constant, $\bar{r}_p = (r_{out} + r_{in})/2$ the mean pore radius, where r_{out}

and r_{in} refer to the outer and inner leaflets of the bilayer, respectively, α is a material parameter; $(1 \le \alpha \le 6)$[24,25] and $\xi = (r_{out} - r_{in})/(r_{out} + r_{in})$. For a typical value of $\bar{r}_p = 0.35$ nm,[21] the pore edge contains seven lipid molecules in the outer leaflet and five lipid molecules in the inner pore leaflet; hence, $\xi = 0.352$. Note that the value of $\bar{r}_p = 0.35$ nm is smaller than the mean length $r_h \approx 0.4$ nm of a lipid headgroup. Nevertheless, since the pore is filled with water, the overall surface membrane area is increased by the amount $\pi\bar{r}_p^2$ due to the local redistribution of lipids in the inner and outer bilayer leaflets.

To connect $\Delta_r G_{ADE}$ with the pore fraction f_p, we recall the formation of membrane pores in terms of the state transition C $\rightleftharpoons$ (P). Since the extent of MEP is usually very small, $f_p = [(P)]/([(P)] + [C]) \ll 1$,[2,3,13] the equilibrium constant $K_p = [(P)]/[C] = f_p/(1 - f_p)$ is approximated by $K_p \approx f_p$. Hence, we have:[6]

$$f_p \approx K_p = K_p^0 \exp[B_H a^{-1}] \tag{13}$$

where the constant $K_p^0 = K_p(a^{-1} = 0)$ covers the remaining thermodynamical, mechanical, and electrical energy terms at zero membrane curvature. The parameter B_H is given by

$$B_H = -\frac{\Delta_r G_{ADE}}{RTa^{-1}} = \frac{64\pi^2\alpha\kappa\bar{r}_p^{\,2}\cdot\xi}{dk_B T} \tag{14}$$

where $R = k_B N_A$ is the gas constant. In our case, f_p depends solely on a^{-1}. Note that eqs 13 and 14 are derived for spherical vesicles. However, the electrooptical results in terms of p indicate a fairly strong vesicle elongation (Figure 1b). In the pole caps of elongated vesicles, the membrane field increases relative to spherical vesicles of equal volume, whereas in the equatorial region of elongated vesicles the field strength decreases. Therefore, the parameter K_p^0, which includes the electric polarization energy term, is not a constant during vesicle elongation. However, the explicit calculation of the θ distribution of the membrane field in an elongated vesicle shows that K_p^0 decreases maximal by 9.2% at $p = 1.68$; see eq C6 of the Appendix and Table 1. In any case, this decrease alone cannot rationalize the effect of membrane curvature on MEP. The effect of the vesicle elongation on f_p due to changes in the membrane field and curvature can be analytically corrected. Already a visual inspection of the values of f_p, recalculated for spherical vesicles in Figure 7a, shows that the spherical approximation applies.

Using eq 13, the analysis of the data (Figure 7a) leads to $K_p^0 = (1.2 \pm 0.1) \times 10^{-3}$ and $B_H = 81 \pm 5$ nm^{-1}, suggesting that, at $\Delta\varphi^N = -0.3$ V and $a^{-1} = 0$ (planar membrane), only the small amount of 0.12% of the membrane area is covered by pores. The value of $B_H = 81$ nm^{-1} indicates that the formation of one conical average pore, e.g., of $\bar{r}_p = 0.35$ nm in a vesicle of $a = 25$ nm leads to the local dissipation of the Gibbs free energy of $\Delta_r G_{ADE}/N_A = -B_H a^{-1} k_B T = -3.2 k_B T$. At the larger vesicle radius $a = 170$ nm there is less curvature and the energy release is correspondingly smaller: $\Delta_r G_{ADE}/N_A = -0.5 k_B T$. Insertion of $\kappa = 2.95 \times 10^{-20}$ J and $\alpha = 2.0$[24] into eq 14 yields the mean pore radius $\bar{r}_p = 0.35$ nm, consistent with previous estimates.[21] Note that the constant value of B_H, required to describe data on f_p in Figure 7a, does not contradict the dependence of κ on the radius a (Figure 5b). Equation 14 shows that B_H is proportional to the product $\alpha\kappa\bar{r}_p^2\xi$, which remains constant, whereas the parameters α, κ, $\bar{r}_p$, and ξ may change independently with increasing radius.

The analysis of the relaxation rates $\tau_p^{-1} = \tau_{II}^{-1}$ of the second relaxation phase (Figure 7b) using the Arrhenius-like ansatz, $\tau_p^{-1} = \tau_0^{-1} \exp[b_H a^{-1}]$, yields the parameters $\tau_0^{-1} = 0.037 \pm 0.003$ μs^{-1} and $b_H = 84 \pm 5$ nm^{-1}. Hence, $b_H \approx B_H$, or the activation energy of curvature-driven electroporation $b_H a^{-1} RT = 3.3RT$ is thus numerically comparable with $-\Delta_r G_{ADE} = 3.2RT$.

Conclusion

The physical−chemical analysis of the turbidity relaxations of small unilamellar lipid vesicles of different sizes ($25 \le a$/nm ≤ 170) measured at the same transmembrane potential ($\Delta\varphi^N = -0.3$ V, $t_E = 10$ μs) quantitatively demonstrates that for these conditions there are major vesicle elongations resulting from stretching and smoothing of the membrane under Maxwell stress, as well as membrane electroporation without measurable reduction of intravesicular volume. Because of the less dense packing order of the lipids in smaller vesicles, the water content of the membrane is larger, whereas the refractive index (n) and the bending rigidity (κ) are smaller than in the larger vesicles. Increased membrane curvature ($H = 2/a$) greatly increases the extent (f_p) and relaxation rate (τ_p^{-1}) of membrane electroporation. The effect of H on f_p is quantified by the decrease in the area difference elasticity energy during formation of electropores.

Summing up, smaller vesicles can be electro-elongated easier, because the smaller bending rigidity and larger pore fraction. The new analytical expressions derived here for vesicle electrodeformation generalize the previous equation of Helfrich[26] for the case of membrane stretching and smoothing of undulations. The novel approach permits to determine the electroporative increase in the membrane surface area separately from that of membrane stretching and smoothing, by analyzing the kinetics of electrodeformation of vesicles and, potentially, of biological cells. Finally, a practical suggestion to experimentators: *to effectively electroporate, curve the membrane!*

Acknowledgment. We thank the Deutsche Forschungsgemeinschaft for grant Ne 227/9-3, /9-4, the ministry MSWF of the land NRW for grant Elminos, the Fonds Chemie and the European Union, Brussels, for grant QLK3-CT-1999-00484 to E. Neumann.

Appendix

A. Equilibrium Vesicle Elongation in DC Electric Fields. In line with Winterhalter and Helfrich,[27] we describe the ellipsoidal elongation of vesicles with the displacement parameter ζ, which is the increase in the radius a in the direction of E and $\zeta/2$ is the corresponding decrease of a in the orthogonal direction. Accordingly, the longest and shortest principal axes of the spheroid are $c = a + \zeta$ and $b = a - \zeta/2$, respectively. For a DC electric field E and for small vesicle deformations ($\zeta \ll a$), the surface energy density of displacements of the membrane patches by the electric Maxwell stress is given by

$$\Delta g_{field}(\zeta) = g_{field}(\zeta) - g_{field}(0) = -(3/20)\epsilon_o\epsilon_w E^2\zeta \tag{A1}$$

where ϵ_o ($= 8.854 \times 10^{-12}$ C^2/(J m)) is the vacuum permittivity.

The ellipsoidal vesicle elongation increases the bending energy density by

$$\Delta g_{bend}(\zeta) = g_{bend}(\zeta) - g_{bend}(0) = (12/5)\kappa\zeta^2/a^4 \tag{A2}$$

Extending the classical theory,[27] the membrane is allowed to stretch and to smooth the thermal membrane undulations during

vesicle elongation. The corresponding increase $\Delta g_{ss}(\sigma,\zeta) = \Delta(\sigma(\zeta)S(\zeta))$ in the energy density is given by

$$\Delta g_{ss}(\sigma,\zeta) = \Delta\sigma(\zeta) + \frac{\sigma_o \Delta S(\zeta)}{S_0} \qquad \text{(A3)}$$

where $\Delta\sigma = \sigma(\zeta) - \sigma_o$ and $\Delta S(\zeta) = S(\zeta) - S_o$.

The surface area of the elongated spheroid is given by

$$S(\zeta) = 2\pi c^2\left[p(\zeta)^{-2} + \frac{\arcsin(\sqrt{1-p(\zeta)^{-2}})}{p(\zeta)\cdot\sqrt{1-p(\zeta)^{-2}}}\right] \qquad \text{(A4)}$$

where p is the axis ratio of the spheroid, $p = c/b$.

At short electric pulses and small degrees of membrane electroporation there is no efflux of intravesicular medium and the vesicle volume V is constant.[13] The constrain of constant volume leads to $V = (4\pi/3)a^3 = (4\pi/3)c^3/p^2$. Substitution of $c = p^{2/3}a$ into eq A4 yields the relative increase in the membrane area required to elongate a vesicle at constant volume:

$$\frac{\Delta S}{S_0} = \frac{p^{-2/3}}{2} + \frac{p^{1/3}\arcsin(\sqrt{1-p^{-2}})}{2\cdot\sqrt{1-p^{-2}}} - 1 \qquad \text{(A5)}$$

The parameter ζ of the vesicle deformation may be found by minimizing the total energy density change $\Delta g(\zeta)$:

$$\Delta g(\zeta) = \Delta g_{field}(\zeta) + \Delta g_{bend}(\zeta) + \Delta g_{ss}(\zeta) \qquad \text{(A6)}$$

For most practical cases, the increase in the lateral tension $\Delta\sigma(\zeta)$ can be found from eq 4 of the text and eq A5. The equilibrium value ζ_o corresponding to a minimum of $\Delta g(\zeta)$ can be found numerically, e.g., by Mathematica 4. If $\Delta\sigma(\zeta)$ is given by eq 7, ζ_o can be calculated analytically by setting $d(\Delta g(\zeta))/d\zeta = 0$. Differentiation of the eqs A1, A2, and A3 yields, respectively:

$$d(\Delta g_{field}(\zeta))/d\zeta = -(3/20)\epsilon_o\epsilon_w E^2 \qquad \text{(A7)}$$

$$d(\Delta g_{bend}(\zeta))/d\zeta = (24/5)\kappa\zeta/a^4 \qquad \text{(A8)}$$

$$d(\Delta g_{ss}(\zeta))/d\zeta = \sigma_o\left[\frac{K}{1 + K/(L\sigma_o)} + 1\right]\left(d\left(\frac{\Delta S(\zeta)}{S_o}\right)/d\zeta\right) \qquad \text{(A9)}$$

For the cases where the first power term ζ/a^2 in $(d(\Delta S)/d\zeta)/S_o$ is sufficient, the approximation

$$d(\Delta g_{ss}(\zeta))/d\zeta \approx \sigma_o\frac{8\pi\kappa(K+\sigma_o) + k_BTK}{8\pi\kappa\sigma_o + k_BTK}\frac{3}{4}\frac{\zeta}{a^2} \qquad \text{(A10)}$$

holds true.

After substitution of the eqs A7, A8, and A10 into eq A6, the solution for $d(\Delta g(\zeta))/d\zeta = 0$ yields the equilibrium value of the membrane displacement:

$$\zeta_o \approx \frac{\epsilon_o\epsilon_w E^2 a^4}{32\kappa + 5\sigma_o a^2\frac{8\pi\kappa(K+\sigma_o) + k_BTK}{8\pi\kappa\sigma_o + k_BTK}} \qquad \text{(A11)}$$

Note that at $\sigma_o = 0$, eq A11 coincides with eq 21 of Winterhalter and Helfrich[27] at zero spontaneous curvature and membrane conductivity.

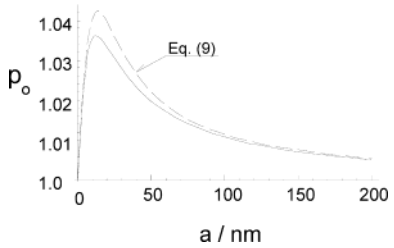

Figure 8. Equilibrium axis ratio p_o as a function of the vesicle radius a at the same (nominal) transmembrane potential $\Delta\varphi^N = -1.5Ea = -0.3$ V, $\kappa = 2.3\cdot10^{-19}$ J, $K = 0.41$ Nm^{-1}, and $\sigma_o = 5\ \mu$N m^{-1} calculated with the exact eq 8 (solid line) and with the approximate eq 9 (dashed line).

Rearrangement of $p = c/b = (a + \zeta)/(a - \zeta/2)$ and series expansion up to $(p-1)^2$ leads to

$$\zeta = a\frac{p-1}{p/2+1} \approx (2/3)a(p-1) \qquad \text{(A12)}$$

Substitution of eq A12 into eq A11 and reorganization yields eq 9 of the text.

For the radius range $25 \le a/\text{nm} \le 170$ and the field strength range $1.2 \le E/\text{MV m}^{-1} \le 8.0$ and at $\kappa = 2.3 \times 10^{-19}$ J, $K = 0.41$ N m^{-1}, and $\sigma_o = 5\ \mu$N m^{-1},[4] eq 9 yields a good approximation to the exact value of p_o (numerical optimization); see Figure 8. Interestingly, at $\sigma_o > 0$ and $Ea =$ constant, p_0 passes through a maximum as a function of the vesicle radius. Actually, at $Ea =$ constant, the electric polarization energy of a vesicle linearly increases with the radius. At small vesicle radii, $a \ll a_{crit}$, where the critical radius is given by

$$a_{crit} = \sqrt{\frac{6.2\kappa}{\sigma_o\left(1 + \frac{K}{\sigma_o + K/L}\right)}} \qquad \text{(A13)}$$

the bending energy term $W_b = 62\kappa$ in eq 9 dominates over the smoothing and stretching energy term $W_{ss} = 10\sigma_o a^2(1 + K/(\sigma_o + K/L))$; hence, $p_0 \propto a$. At $a \gg a_{crit}$, $W_{ss} \gg W_b$, leading to $p_0 \propto a^{-1}$, rationalizing the reversal in the dependence on a (Figure 8).

The characteristic vesicle deformation time may be estimated from the generalized Stokes force $F = 6\pi\eta a v$, where η is the viscosity of medium (water) and $v = d\zeta/dt$ the velocity of the membrane displacement. Small membrane displacements at the vesicle elongation can be modeled by a displacement of the center of a sphere of radius a under the action of the changing generalized force:

$$F(\zeta) = -S_o d(\Delta g(\zeta))/d\zeta \qquad \text{(A14)}$$

So far as $F(\zeta)$ decreases to zero, while ζ approaches the equilibrium value ζ_o, an estimation for the characteristic time of the elongation is given by Stokes' law in the integral form

$$\tau = 6\pi\eta a\int_0^{\zeta_o(1-e^{-1})}[F(\zeta)]^{-1}d\zeta \qquad \text{(A15)}$$

where $\zeta_e = \zeta_o(1 - e^{-1})$ represents $1/e$ of the total equilibrium displacement ζ_o ($e \approx 2.72$). With eqs A6−A10, the integration of eq A15 yields eq 10 of the text.

B. Membrane Curvature at Vesicle Elongation. Due to electroelongation, the membrane curvature H locally increases in the vesicle pole caps and decreases in the equatorial region. The functional dependence of H on the positional angle θ can be expressed as

$$H(\theta) = \frac{1}{R_m(\theta)} + \frac{1}{R_p(\theta)} \quad \text{(B1)}$$

The meridian R_m and the parallel R_p principal radii, respectively, are given by

$$R_m(\theta) = c\frac{(1 - e^2\cos^2(\theta))^{3/2}}{(1 - e^2)^{1/2}} \quad \text{(B2)}$$

$$R_p(\theta) = c(1 - e^2)^{1/2}(1 - e^2\cos^2(\theta))^{1/2} \quad \text{(B3)}$$

where e is the eccentricity: $e = \sqrt{1-(b/c)^{-2}}$.

For an elongated vesicle, the θ-average $\langle H\rangle$ of $H(\theta)$ is defined by

$$\langle H\rangle = 0.5\cdot\int_0^{\pi} H(\theta)\sin(\theta)\mathrm{d}\theta \quad \text{(B4)}$$

and the spherical equivalent radius is specified as $a_{eq} = 2/\langle H\rangle$. Note that for a sphere of radius a we have $\langle H_0\rangle = \langle H\rangle = H = 2/a$ and $a_{eq} = a$. The relative increase in the θ-average curvature $\Delta\langle H\rangle/\langle H_0\rangle$ is defined by

$$\frac{\Delta\langle H\rangle}{\langle H_0\rangle} = \frac{\langle H\rangle - \langle H_0\rangle}{\langle H_0\rangle}, \quad \text{(B5)}$$

The values of a_{eq} and $\Delta\langle H\rangle/\langle H_0\rangle$ for vesicle elongation at constant volume are summarized in Table 1.

C. Field Distribution in Elongated Vesicles. For an elongated vesicle, oriented with the long axis c along with the external field vector E, the field-induced potential difference can be written in the form (see, e.g., ref 28)

$$\Delta\varphi_m = -\frac{E}{1 - n_{||}}\cdot\frac{cb\cos(\theta)}{\sqrt{c^2\sin^2(\theta) + b^2\cos^2(\theta)}} \quad \text{(C1)}$$

where

$$n_{||} = \frac{1 - e^2}{2e^3}\left(\ln\frac{1 + e}{1 - e} - 2e\right) \quad \text{(C2)}$$

is the depolarization factor of the prolate ellipsoid ($c > b$). Substitution of eq C2 into eq C1 yields explicitly

$$\Delta\varphi_m = -\frac{c^2 - b^2}{c - \frac{b^2}{2\sqrt{c^2 - b^2}}\ln\frac{c + \sqrt{c^2 - b^2}}{c - \sqrt{c^2 - b^2}}}\cdot\frac{b\cos(\theta)E}{\sqrt{c^2\sin^2(\theta) + b^2\cos^2(\theta)}} \quad \text{(C3)}$$

Equation C3 essentially differs from that derived for $\Delta\varphi_m$ by Gimsa and Wachner[28] and by Kotnik and Miklavcic.[29] Note that eq C3 does not result in $\Delta\varphi_m = 0$ for the case $c = b$ (spherical vesicle, $p = 1$), yet in the limit case of a sphere, where $c = b = a$, eq C3 reduces to the well-known expression: $\Delta\varphi_m = -1.5a\,|\cos(\theta)|E$.[2]

For vesicle deformations at constant intravesicular volume V, i.e., no electrolyte efflux, the equality $a^3 = cb^2$ holds. Inserting this equality and $p = c/b$ into eq C3 we obtain

$$\Delta\varphi_m = -\frac{p^{2/3}}{1 - \frac{p^{-2}}{2(\sqrt{1 - p^{-2}})^3}\left(\ln\frac{1 + \sqrt{1 - p^{-2}}}{1 - \sqrt{1 - p^{-2}}} - 2\cdot\sqrt{1 - p^{-2}}\right)}\cdot\frac{a\cos(\theta)E}{\sqrt{p^2\sin^2(\theta) + \cos^2(\theta)}} \quad \text{(C4)}$$

Pore Fraction during Vesicle Elongation at Constant Volume. Since the extent of membrane electroporation is approximately proportional to the square of the induced transmembrane potential (i.e., polarization energy), the total surface fraction f_p of membrane electropores is proportional to the θ-average:

$$\langle\Delta\varphi_m^2\rangle = 0.5\int_0^{\pi}\Delta\varphi_m^2(\theta)\sin(\theta)\mathrm{d}\theta \quad \text{(C5)}$$

The relative change in the equilibrium constant K_p^0 due to vesicle elongation can be expressed by

$$\frac{\Delta K_p^0}{K_p^0} = \frac{K_p(p) - K_p(p = 1)}{K_p(p = 1)} = \frac{\Delta f_p}{f_p} = \frac{f_p(p) - f_p(p = 1)}{f_p(p = 1)} = \frac{\langle\Delta\varphi_m^2(p)\rangle - \langle\Delta\varphi_m^2(p = 1)\rangle}{\langle\Delta\varphi_m^2(p = 1)\rangle} \quad \text{(C6)}$$

Substitution of eq C4 into eq C5 at a constant value of the product $aE = 0.2$ V, for example, and integration yields values of $\Delta K_p^0/K_p^0$ ($p = 1$) at different vesicle radii (Table 1).

Glossary

K	membrane stretching modulus (N m^{-1})
K_p	equilibrium constant of membrane electroporation
d	membrane thickness
k_B	Boltzmann constant
N_A	Avogadro constant
T	the absolute temperature
ΔS	increase in the membrane surface area
ΔS_{ss}	increase of area due to the membrane stretching and smoothing of undulations
ΔS_p	increase of membrane area due to the electropores
S_0	initial membrane surface area (at $E = 0$)
S	membrane area in the field E
a	radius of vesicle
$p = c/b$	axis ratio of spheroidal vesicle
E	electric field strength (V m^{-1})
σ	(as superscript) polarization angle
σ	membrane lateral tension (N m^{-1})
σ_0	initial membrane lateral tension (at $E = 0$)
κ	membrane bending rigidity (J)

References and Notes

(1) Sackmann, E. *FEBS Lett.* **1994**, *346*, 3.
(2) Neumann, E.; Kakorin, S.; Toensing, K. *Bioelectrochem. Bioenerg.* **1999**, *48*, 3.
(3) Neumann, E.; Kakorin, S.; Toensing, K. *Faraday Discuss.* **1998**, *111*, 111.
(4) Kummrow, M.; Helfrich W. *Phys. Rev. A* **1991**, *44*, 8356.
(5) Swairjo, M. A.; Seaton, B. A.; Roberts, M. F. *Biochim. Biophys. Acta* **1994**, *1191*, 354.
(6) Neumann, E.; Kakorin, S. *Biophys. Chem.* **2000**, *85*, 249.

(7) Correa, N. M.; Schelly, Z. *J. Phys. Chem. B* **1998**, *102*, 9319.
(8) Correa, N. M.; Schelly, Z. *Langmuir* **1998**, *14*, 5802.
(9) Toensing, K.; Kakorin, S.; Neumann, E.; Liemann, S.; Huber, R. *Eur. Biophys. J.* **1997**, *26*, 307.
(10) Kakorin, S.; Redeker, E.; Neumann, E. *Eur. Biophys. J.* **1998**, *27*, 43.
(11) Kakorin, S.; Neumann, E. *Ber. Bunsen-Ges. Phys. Chem.* **1998**, *102*, 670.
(12) Farafonov, V. G.; Voshinnikov N. V.; Somsikov V. V. *App. Optics* **1996**, *35*, 5412.
(13) Griese, T.; Kakorin, S.; Neumann, E. *Phys. Chem. Chem. Phys.* **2002**, *4*, 1217.
(14) Helfrich, W.; Servuss, R.-M. *IL Nuovo Cimento* **1984**, *3D*, 137.
(15) Klösgen, B.; Helfrich, W. *Eur. Biophys. J.* **1993**, *22*, 329.
(16) Cevc, G.; Seddon, J. In *Phospolipid Handbook*; Cevc, G., Ed.; Marcel Dekker, Inc.: New York, 1993; p 351.
(17) Komura, S. *Vesicles;* Library of Congress Cataloguing-in-Publication Data: New York, 1996; Chapter 6.
(18) Argharian, N.; Schelly, Z. A. *Biochim. Biophys. Acta* **1999**, *1418*, 295.
(19) Goetz, R.; Gomper, G.; Lipowsky, R. *Phys. Rev. Lett.* **1999**, *82*, 221.
(20) Neumann E. *Electroporation and Electrofusion in Cell Biology*; Plenum Press: New York, 1989; Chapter 4.
(21) Kakorin, S.; Stoylov, S. P.; Neumann, E. *Biophys. Chem.* **1996**, *58*, 109.
(22) Tekle, E.; Astumian, R. D.; Friauf, W. A.; Chock, P. B. *Biophys. J.* **2001**, *81*, 960.
(23) Chang, D. C.; Reese, Th. S. *Biophys. J.* **1990**, *58*, 1.
(24) Seifert, U.; Lipowsky, R. *Structure and Dynamics of Membranes*, 1A; Elsevier: Amsterdam, 1995; Chapter 8.
(25) Wiese, W.; Harbich, W.; Helfrich, W. *J. Phys. Condens. Matter* **1992**, *4*, 1647.
(26) Helfrich, W. *Z. Naturforsch.* **1974**, *29c*, 182.
(27) Winterhalter, M.; Helfrich, W. *J. Coll. Interface Sci.* **1988**, *122*, 583.
(28) Gimsa, J.; Wachner, D. *Eur. Biophys. J.* **2001**, *30*, 463.
(29) Kotnik, T.; Miklavcic, D. *Biophys. J.* **2000**, *79*, 670.